

Reply to referee (2)'s comments on NHESS-2024-203:

We would like to thank the reviewer for the invaluable comments and suggestions. Here are our responses to the referee's comments.

Major comments

The study proposes an adaptive hydrometeor retrieval scheme, which adaptively combines “temperature-based” and “background hydrometer-dependent” methods to improve analyses and forecasts of two real cases occurred during June 2020 and August 2018. However, the manuscript lacks more details about the retrieval scheme itself. Specifically, it would be helpful to provide a more detailed explanation of how the two methods are combined, including the criteria or algorithm used for their weighting. Additionally, English writing needs to be further improved.

Reply: Thanks. It is revised with “

2.3.2 The “Background hydrometer-dependent” method

It is found that hydrometeor weights derived from the background field vary with individual weather conditions, which helps to reduce errors resulting from fixed coefficients in Chen et al. (2020, 2021). The specific process of calculating proportions is as follows:

(1) Compute the average equivalent radar reflectivity of each hydrometeor ($\overline{Z_{x(k,ref_i)}}$) in different reflectivity ranges (ref_i) and model layers (k) based on the background field statistics. The reflectivity ranges are usually set as follows: $ref_1 < 15$ dBZ, 15 dBZ $\leq ref_2 < 25$ dBZ, 25 dBZ $\leq ref_3 < 35$ dBZ, 35 dBZ $\leq ref_4 < 45$ dBZ, $ref_5 \geq 45$ dBZ.

(2) Calculate the weight ($C_{x(k,ref_i)}$) of each hydrometeor in the background field.

$$\overline{Z_{total(k,ref_i)}} = \overline{Z_{r(k,ref_i)}} + \overline{Z_{s(k,ref_i)}} + \overline{Z_{g(k,ref_i)}}. \quad (10)$$

(3) Divide radar reflectivity observations based on the weights ($C_{x(k,ref_i)}$) derived from Step 2. If the background field has missing data, the calculated climatological mean for one month will be used instead.

2.3.3 The blending method

The blending method aims to utilize the two methods of partitioning hydrometeors accordingly to retrieve multi-hydrometer more reasonably in radar reflectivity indirect assimilation. Firstly, calculate the standard deviation σ of each hydrometeor content in the model grid and its

surrounding background grids. If the standard deviations of the retrieved hydrometeors of the two schemes are less than 2σ , it means that the retrieved hydrometeors are consistent with the local structure of the background. Therefore, the hydrometeor content is calculated by the following formulas:

$$\beta = \frac{\delta_t^2}{\delta_t^2 + \delta_b^2}, \quad (11)$$

$$C_x = \beta C_x^b + (1 - \beta) C_x^t. \quad (12)$$

δ_t^2 represents the deviation between the hydrometeor content of the background field and the retrieved hydrometeor content based on the “temperature-based” scheme. δ_b^2 is the deviation between the hydrometeor content of the background field and the retrieved hydrometeor by the “background hydrometer-dependent” scheme. C_x^t and C_x^b are the weights calculated by the “temperature-based” and “background hydrometer-dependent” methods, respectively. β means the proportion of the results calculated by “background hydrometer-dependent” method.” In the section 2. Besides, the writing has been further improved.

Minor comments

1. The manuscript lacks a detailed description of the used radars in the two case studies.

Reply: Thanks. Added as “Besides, the specific flowchart is presented in the Fig. 2. The radar observations used in two cases undergo a series of preprocessing and quality control procedure, including anomaly detection, velocity de-aliasing, and so on. The observation errors of radar radial velocity and radar reflectivity are set to 2 m s^{-1} and 5 dBZ, respectively.” in the section 3.

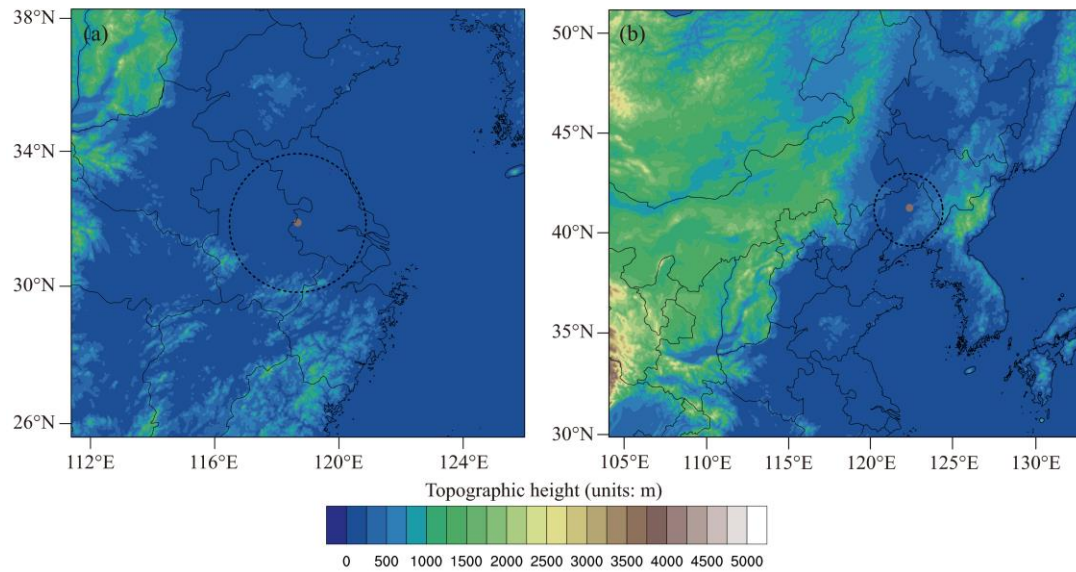


Fig. 1. The simulated area of (a) Case 1 and (b) Case 2, with the detecting ranges of the Nanjing radar and Shenyang Radar. Both radars are S-band Doppler radars with a maximum coverage range of 230 km. The radial velocity and reflectivity observations have range resolutions of 250 m and 1000 m, respectively.

2. Due to the critical role of water vapor in the development of strong convection, it is necessary to clarify whether water vapor is assimilated and how it is assimilated in the method section.

Reply: Thanks.

Added as “Therefore, the indirect assimilation method is utilized in the study. The indirect method assimilates the retrieved water vapor and hydrometeors from the radar reflectivity observations. Following Wang et al. (2013), it is assumed that when the radar reflectivity exceeds a certain threshold, the relative humidity reaches 100%. The threshold is set to 30 dBZ in this study. The saturation water vapor at that point is then calculated and assimilated as a pseudo observation.

For retrieving hydrometeors from radar reflectivity, it is required to determine the proportion of each hydrometeor in radar reflectivity observation. At present, there are two methods to obtain the proportion of each hydrometeor.” in the section 2.3.

3. Comparing Fig. 10 and Fig. 11, it seems that the vertical distribution of hydrometeor and radar reflectivity do not match.

Reply: Sorry, we misplaced the picture. The correct pictures are as follows.

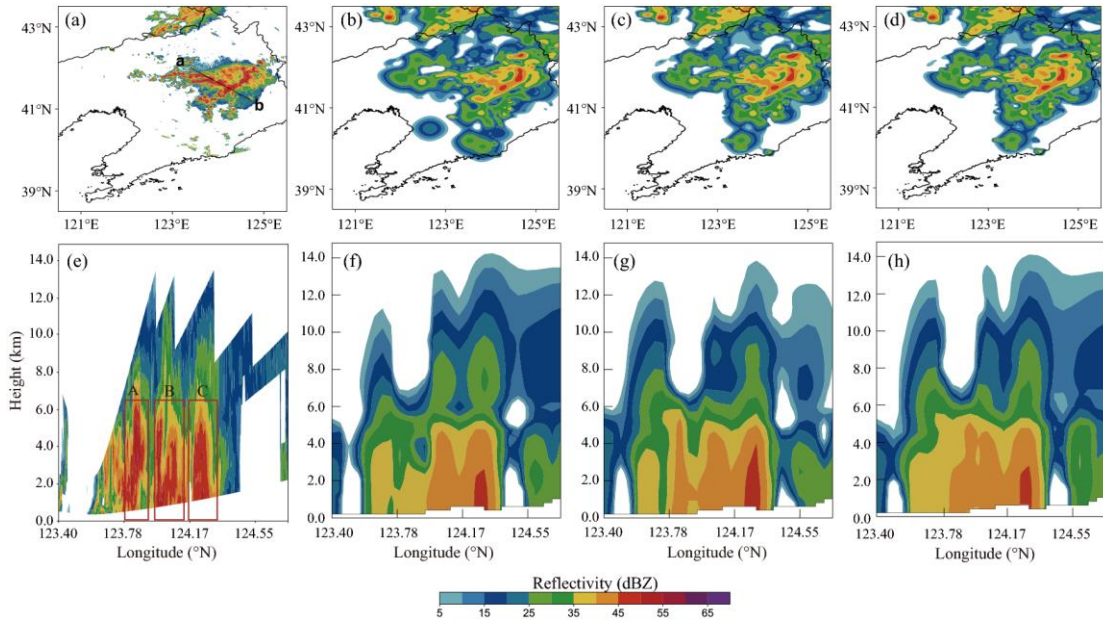


Fig. 10. The composite reflectivity at 2100 UTC for (a) observation, (b) EXP_temp, (c) EXP_bg, (d) EXP_temp-bg, accompanied by the vertical cross sections for (e) observation, (f) EXP_temp, (g) EXP_bg, (h) EXP_temp-bg along the line ab. The vertical cross section location at 2100UTC is shown by the line ab in the Fig. 10a. The labels in the Fig. 10e present the convection locations.

4. In the second case study, the evaluation of all experiments is primarily qualitative, lacking a thorough quantitative assessment.

Reply: Thanks. Added as “Fig. 15 shows ETS values of 1-h accumulated precipitation for EXP_temp, EXP_bg, and EXP_temp-bg. For the thresholds of 2.5 mm/h, the precipitation forecasts of EXP_temp-bg generally exhibit superior quality. The experiment EXP_temp keeps the worst for the ETS scores among the three sets of experiments. At thresholds of 10 mm/h, the score of EXP_temp-bg gradually increases in the later stage of forecast. The scores indicate that the blending method is able to improve the precipitation forecast skill.” in the section 4.2.

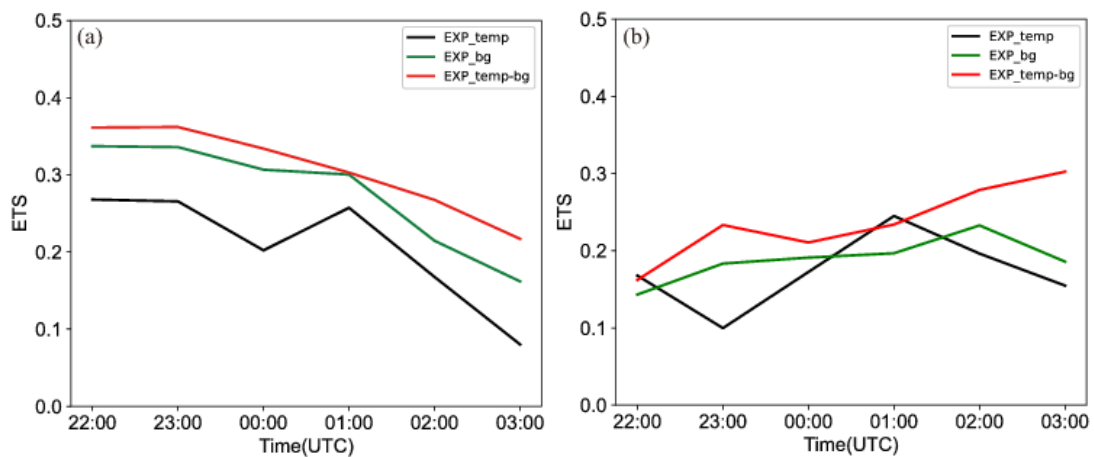


Fig. 15. ETS of three DA experiments for the thresholds of (a) 2.5 mm/h, (b) 10 mm/h.

5. Line 316, “However, it does not exist in the other two experiments” the sentence is not clearly expressed.

Reply: Thanks. It is modified for “For schemes associated with the background, the weights assigned to different hydrometeors vary dynamically with the background field. Therefore, the fixed coefficient does not exist in the other two experiments (EXP_bg and EXP_temp-bg)” in the section 4.2.

6. Line 368, “As shown in Fig. 9c and d”?

Reply: Thanks. It is modified for “As shown in Fig. 14c and d, the patterns of heavy precipitation areas are similar in EXP_bg and EXP_temp-bg.”

7. It is beneficial to add a water vapor cross section in the second case similar to Figure 6. Providing such a cross section would help explain the impact of the different retrieval scheme on moisture distribution.

Reply: Thanks. The figure displays the vertical profiles of the relative humidity, radar reflectivity and wind fields at 2200 UTC 6 August.

the cross sections from all experiments indicate the presence of saturated water vapor columns between 123.8°E and 125.2°E, accompanied by a strong updraft assisting the transport of moisture from the lower levels to the upper levels.

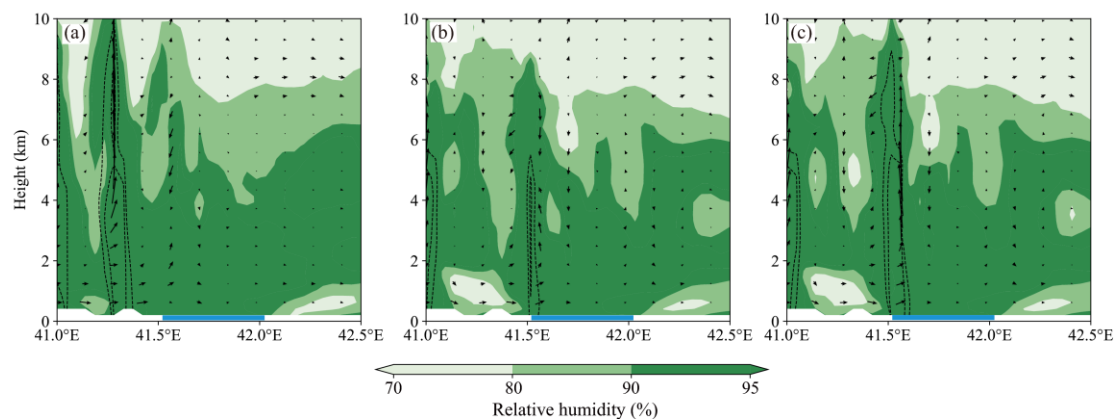


Fig. The cross sections of relative humidity (shading; units: %), radar reflectivity (black contours starting at 40 dBZ; units: dBZ), and wind vectors for (a) EXP_temp, (b) EXP_bg and (c) EXP_temp-bg along the longitude line of 123.6°E. These are 1-hour forecasts initialized at 2100 UTC. The blue rectangle at the bottom of the figure shows the strong echo area.